Quaternary Geochronology 19 (2014) 173–180

Contents lists available at SciVerse ScienceDirect

Quaternary Geochronology

journal homepage: www.elsevier.com/locate/quageo

Research paper

Discordance between cosmogenic nuclide concentrations in amalgamated sands and individual fluvial pebbles in an arid zone catchment

Alexandru T. Codilean [a,*], Cassandra R. Fenton [b,1], Derek Fabel [a], Paul Bishop [a], Sheng Xu [c]

[a] School of Geographical and Earth Sciences, The University of Glasgow, Glasgow G12 8QQ, UK
[b] NERC Cosmogenic Isotope Analysis Facility, Scottish Universities Environmental Research Centre, East Kilbride G75 0QF, UK
[c] AMS Laboratory, Scottish Universities Environmental Research Centre, East Kilbride G75 0QF, UK

ARTICLE INFO

Article history:
Received 22 December 2011
Received in revised form
20 March 2012
Accepted 9 April 2012
Available online 21 April 2012

Keywords:
Beryllium-10
Aluminium-26
Neon-21
Cosmogenic nuclide
Grain size bias
Namibia

ABSTRACT

Based on cosmogenic ^{10}Be and ^{26}Al analyses in 15 individual detrital quartz pebbles (16–21 mm) and cosmogenic ^{10}Be in amalgamated medium sand (0.25–0.50 mm), all collected from the outlet of the upper Gaub River catchment in Namibia, quartz pebbles yield a substantially lower average denudation rate than those yielded by the amalgamated sand sample. ^{10}Be and ^{26}Al concentrations in the 15 individual pebbles span nearly two orders of magnitude (0.22 ± 0.01 to $20.74 \pm 0.52 \times 10^6$ ^{10}Be atoms g^{-1} and 1.35 ± 0.09 to $72.76 \pm 2.04 \times 10^6$ ^{26}Al atoms g^{-1}, respectively) and yield average denudation rates of ~0.7 m Myr^{-1} (^{10}Be) and ~0.9 m Myr^{-1} (^{26}Al). In contrast, the amalgamated sand yields an average ^{10}Be concentration of $0.77 \pm 0.03 \times 10^6$ atoms g^{-1}, and an associated mean denudation rate of 9.6 ± 1.1 m Myr^{-1}, an order of magnitude greater than the rates obtained for the amalgamated pebbles. The inconsistency between the ^{10}Be and ^{26}Al in the pebbles and the ^{10}Be in the amalgamated sand is likely due to the combined effect of differential sediment sourcing and longer sediment transport times for the pebbles compared to the sand-sized grains. The amalgamated sands leaving the catchment are an aggregate of grains originating from all quartz-bearing rocks in all parts of the catchment. Thus, the cosmogenic nuclide inventories of these sands record the overall average lowering rate of the landscape. The pebbles originate from quartz vein outcrops throughout the catchment, and the episodic erosion of the latter means that the pebbles will have higher nuclide inventories than the surrounding bedrock and soil, and therefore also higher than the amalgamated sand grains. The order-of-magnitude grain size bias observed in the Gaub has important implications for using cosmogenic nuclide abundances in depositional surfaces because in arid environments, akin to our study catchment, pebble-sized clasts yield substantially underestimated palaeo-denudation rates. Our results highlight the importance of carefully considering geomorphology and grain size when interpreting cosmogenic nuclide data in depositional surfaces.

1. Introduction

In situ-produced cosmogenic nuclide analyses in both modern and buried sediment are widely used to quantify modern- and palaeo-denudation rates integrated over a wide range of spatial and temporal scales (e.g., von Blanckenburg, 2005; Dunai, 2010; Portenga and Bierman, 2011). Such studies assume that the sediment sample comprises grains originating from all parts of a catchment and that it records the average denudation rate of the sediment's source (Bierman and Steig, 1996; Brown et al., 1995; Granger et al., 1996). The latter assumption implies that the cosmogenic nuclide concentration of the sample, and so the inferred denudation rate, do not depend on grain size. Numerous studies have found no dependence of nuclide concentration on grain size (e.g., Granger et al., 1996; Clapp et al., 2000, 2002; Schaller et al., 2001; Ouimet et al., 2009; Palumbo et al., 2010; see Supplementary Data), but substantial grain size effects have been observed in a few, mostly humid, environments, including Puerto Rico (Brown et al., 1998), the Appalachian Mountains (Matmon et al., 2003), the Olympic Mountains (Belmont et al., 2007), and the Amazon Basin (Wittmann et al., 2011).

* Corresponding author. Present address: Deutsches GeoForschungsZentrum GFZ, Section 3.4: Earth Surface Geochemistry, Potsdam D-14473, Germany. Tel.: +49 331 288 28612; fax: +49 331 288 2852.
E-mail address: codilean@gfz-potsdam.de (A.T. Codilean).
[1] Present address: Deutsches GeoForschungsZentrum GFZ, Section 4.2: Inorganic and Isotope Geochemistry, Potsdam D-14473, Germany.

1871-1014/$ – see front matter © 2012 Elsevier B.V. All rights reserved.
doi:10.1016/j.quageo.2012.04.007

A possible grain size effect can also be observed in cosmogenic nuclide data from the Gaub River catchment in the arid central-western Namibia (Codilean et al., 2008) (Fig. 1). Codilean et al. (2008) established the spatial pattern of denudation in the Gaub using in situ-produced cosmogenic ^{10}Be (^{10}Be$_c$) in amalgamated sand samples (0.25–0.50 mm), showing that the spatial distribution of denudation is reflected in the shape of the frequency distribution of cosmogenic ^{21}Ne (^{21}Ne$_c$) concentrations in 32 quartz pebbles (16–21 mm) randomly collected from the catchment outlet (Fig. 1C). Although the spatial pattern of denudation implied by the ^{21}Ne$_c$ in the pebbles is consistent with Codilean et al.'s (2008) ^{10}Be$_c$ data from amalgamated sand samples (Fig. 1), when amalgamated the ^{21}Ne$_c$ concentrations in the pebbles yield a substantially lower average denudation rate of ~1 m Myr^{-1} as compared to the ~12 m Myr^{-1} determined using the ^{10}Be$_c$ in the sand (Bierman and Caffee, 2001; Codilean et al., 2008). Identifying the cause of this apparent discrepancy between the ^{10}Be$_c$ in the sand and ^{21}Ne$_c$ in the pebbles is hindered by the fact that it involves two separate isotopic systems. If the low ^{10}Be$_c$ in the sand (relative to the ^{21}Ne$_c$ in the pebbles) is not a grain-size effect, it could indicate radioactive decay of ^{10}Be$_c$ during long-term sediment storage, in both the colluvial and fluvial systems, at depths sufficient for cosmogenic nuclide production to cease. Conversely, the relatively high ^{21}Ne$_c$ concentrations in the pebbles, relative to the ^{10}Be$_c$ in the sand, could indicate the presence of excess non-cosmogenic ^{21}Ne that has not been identified during measurement (cf. Niedermann, 2002).

To establish the cause of this apparent grain size bias in the Gaub River catchment, we measured cosmogenic ^{10}Be and ^{26}Al (^{26}Al$_c$) in 15 of Codilean et al.'s (2008) 32 pebbles (Fig. 1C). In the case of a mismatch between the ^{10}Be$_c$ and ^{21}Ne$_c$ in the pebbles, measurements of ^{26}Al$_c$ will determine whether this is the result of radioactive decay of ^{10}Be$_c$ during long-term sediment storage, or the presence of excess non-cosmogenic ^{21}Ne. In addition, to better constrain the spatial pattern of denudation and to confirm that the sediment leaving this catchment is a mixture of grains originating from all parts of the catchment, we complemented Codilean et al.'s (2008) ^{10}Be$_c$ amalgamated sand data with a further eight samples: seven from tributaries and a further sample from the catchment outlet (Fig. 1A).

2. Field setting

The Gaub is a tributary of the ~15,500 km^2 Kuiseb River, one of the major ephemeral rivers systems draining western Namibia. The study catchment has an area of ~1200 km^2 and the geomorphology is that of a high elevation passive margin with an extensive low-relief upland region and a highly dissected, high-relief zone marking the Great Escarpment. Quartzites and granites of the Rehoboth group (1650–1860 Myr) and Sinclair group (1050–1400 Myr) are the dominant rock types in the study catchment (Ziegler and Stoessel, 1993). Quartz is an abundant component of all lithological units and quartz-vein outcrops are ubiquitous throughout the catchment (Fig. 2).

Overall, denudation rates in central-western Namibia are low, with the steeper escarpment area eroding more rapidly than either the more gently sloping coastal plain or the upland plateau. Cosmogenic nuclide-based bedrock erosion rates average around ~3 m Myr^{-1} on the coastal plain and upland plateau (Bierman and Caffee, 2001; van der Wateren and Dunai, 2001), and the steeper escarpment area is eroding in the proximity of the study catchment at a rate of ~10 m Myr^{-1} (Cockburn et al., 2000). Denudation rates based on ^{10}Be$_c$ analysis of sediment are higher than their bedrock counterparts but exhibit a similar regional pattern: ~8 and ~6 m Myr^{-1} on the coastal plain and upland plateau respectively, and ~16 m Myr^{-1} on the escarpment (Bierman and Caffee, 2001; Bierman et al., 2007; Codilean et al., 2008).

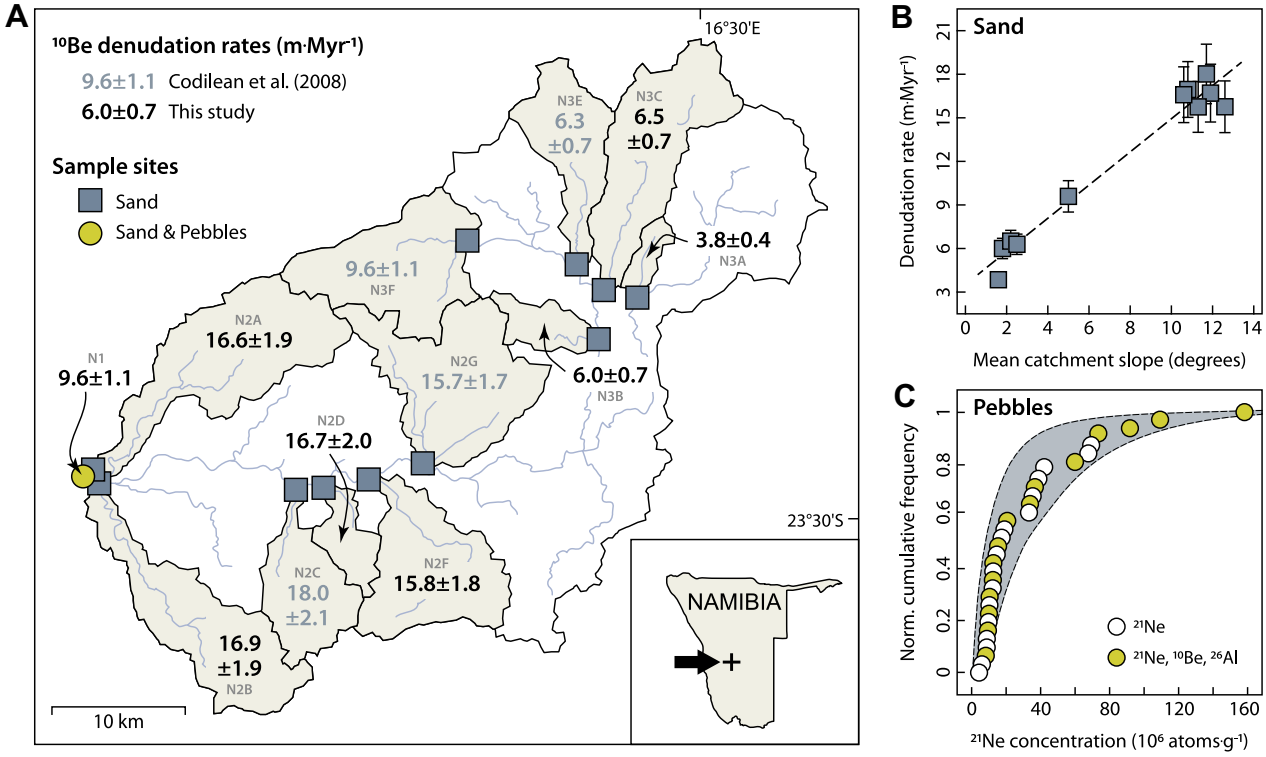

Fig. 1. Field setting and cosmogenic nuclide data. (A) Map of study area showing denudation rates (m Myr^{-1}) inferred from ^{10}Be$_c$ analyses in amalgamated sand samples by Codilean et al. (2008) and this study. (B) Plot of the ^{10}Be$_c$ catchment-wide denudation rates obtained for the 11 Gaub sub-catchments in (A) versus the mean slopes of these sub-catchments. (C) Cumulative frequency distribution plot showing Codilean et al.'s (2008) ^{21}Ne$_c$ concentrations in the 32 pebbles. Circles in yellow indicate the pebbles that were selected for ^{10}Be$_c$ and ^{26}Al$_c$ measurements (this study). (For interpretation of the references to colour in this figure legend, the reader is referred to the web version of this article.)

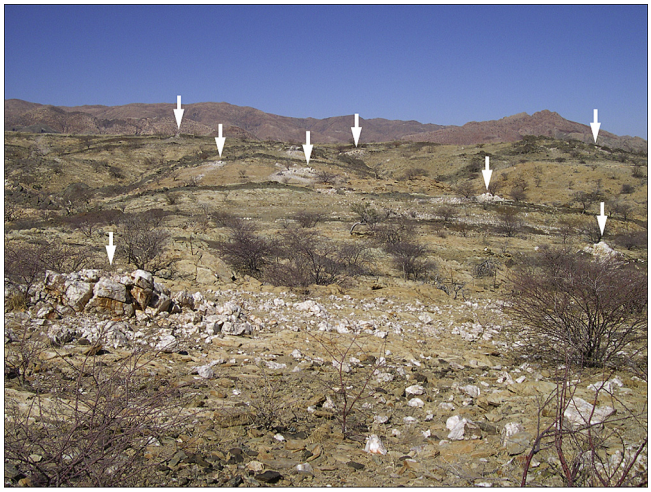

Fig. 2. Typical view of the study area showing the ubiquitous nature of quartz-vein outcrops (white arrows).

3. Methods and data

Quartz samples were prepared according to the procedure described by Wilson et al. (2008) with the following modifications: (1) Inherent Al in quartz after etching was ≤35 ppm; (2) 260 or 320 μg ^{9}Be and 2.46–2.50 mg ^{27}Al were added as carrier to the main solution, and (3) Ti was removed by cation-exchange chromatography using sulphuric acid.

The ^{10}Be/^{9}Be and ^{26}Al/^{27}Al ratios were measured with the 5MV NEC Pelletron accelerator mass spectrometer at SUERC (Freeman et al., 2004) as part of routine Be and Al runs. The measurements are described in detail by Maden et al. (2007), Freeman et al. (2007), Schnabel et al. (2007), and Xu et al. (2010). The NIST SRM4325 standard (with a calibrated ^{10}Be/^{9}Be ratio of 3.06×10^{-11}; Middleton et al., 1993) was used for normalisation, which is 14% higher than the NIST certified value (^{10}Be/^{9}Be $= 2.68 \times 10^{-11}$). To make all subsequent calculations consistent with the updated ^{10}Be half-life of 1.387 ± 0.012 Myr (Chmeleff et al., 2010; Korschinek et al., 2010), the ^{10}Be data were re-normalised to the 2007 KNSTD standard (Nishiizumi et al., 2007). The ^{10}Be/^{9}Be ratios of the full chemistry procedural blanks prepared with the samples were $3.1 \pm 1.0 \times 10^{-15}$ for the amalgamated sands, and $5.3 \pm 0.6 \times 10^{-15}$ and $5.1 \pm 0.6 \times 10^{-15}$ for the pebbles, respectively. This ratio was subtracted from the Be isotope ratios of the samples. Blank-corrected ^{10}Be/^{9}Be ratios of the amalgamated sands ranged from 5.02×10^{-13} to 3.63×10^{-12}, and for the pebbles from 3.2×10^{-14} to 2.07×10^{-12}. One-sigma uncertainties of the SUERC AMS measurement include the uncertainty of the sample measurement, the uncertainty associated with the measurement of the primary standard and the uncertainty of the blank correction. Total one-sigma uncertainties for the concentrations (atoms g^{-1} quartz) determined at SUERC include the one-sigma uncertainty of the AMS measurement and a 2% uncertainty as a realistic estimate for possible effects of the chemical sample preparation which includes the uncertainty of the Be concentration of the carrier solution.

Typical ion currents of ^{27}Al were 250–420 nA. Z92-0222 (donated from PRIME Lab, Purdue University) with a nominal ^{26}Al/^{27}Al ratio of 4.11×10^{-11} was used as primary standard. The measurements of this material agree with the measurements of standard material supplied by K. Nishiizumi (2002, 2004); Z92-0222 is equivalent to the KNSTD standard for Al in the CRONUS-Earth online calculator (Balco et al., 2008). The ^{26}Al/^{27}Al ratios of the processing blanks prepared with the samples ranged from 1×10^{-15} to 2×10^{-15}. An average ratio of 1.7×10^{-15} was subtracted from the Al isotope ratios of the samples. Blank-corrected ^{26}Al/^{27}Al ratios of the samples ranged from 4.5×10^{-14} to 2.3×10^{-12}. One-sigma uncertainties of the SUERC AMS measurement consist of the uncertainty of the sample measurement, the internal uncertainty of the normalization (reproducibility of the measurements of the primary standard) and the uncertainty of the blank correction. One-sigma uncertainties for the concentrations determined at SUERC include the one-sigma uncertainty of the AMS measurement and the one-sigma uncertainty of the determination of total Al with ICP-MS (typically between 2.0% and 2.1%). The uncertainty on the total Al is close to that of the one-sigma uncertainty (2.0%) of the carrier solution that was used in these analyses. The one-sigma uncertainties of the ICP-MS measurements for inherent ^{27}Al concentrations ranged from 2.5 to 3.8%. Expressed ^{10}Be and ^{26}Al AMS analysis uncertainties are consistent with the long-term measurement reproducibility of standard material of similar isotope ratio. The treatment of the uncertainties that contribute to the uncertainty of the ^{26}Al concentration in atoms g^{-1} quartz is described in Roberts et al. (2008).

Catchment wide denudation rates were calculated using the re-normalised (2007 KNSTD) ^{10}Be concentrations, and following the formalism of Schaller et al. (2001) with ^{10}Be$_{\mathbf{c}}$ SLHL production rates of: 4.5 ± 0.5 atoms g^{-1} yr^{-1} for high-energy neutrons, 0.097 ± 0.007 atoms g^{-1} yr^{-1} for slow muons, and 0.085 ± 0.012 atoms g^{-1} yr^{-1} for fast muons. The ^{10}Be$_{\mathbf{c}}$ SLHL production rate for high-energy neutrons was recalculated from Balco et al.'s (2008) ^{10}Be$_{\mathbf{c}}$ calibration-site dataset, using the time-independent altitude/latitude scaling scheme of Dunai (2000) and a ^{10}Be$_{\mathbf{c}}$ half-life of 1.387 ± 0.012 Myr (Chmeleff et al., 2010; Korschinek et al., 2010). The ^{10}Be$_{\mathbf{c}}$ SLHL production rates for muons were taken from Kubik et al. (2009) and are based on Heisinger et al. (2002a,b). All ^{10}Be$_{\mathbf{c}}$ SLHL production rates were corrected for altitude and latitude using the time-independent scaling scheme of Dunai (2000) and for topographic shielding following Codilean (2006). All calculations were performed on a pixel-by-pixel basis using the 90 m SRTM DEM (http://srtm.csi.cgiar.org/). All previously published ^{10}Be$_{\mathbf{c}}$ data that are quoted in the text were also recalculated following the procedure outlined above. We use a ^{21}Ne$_{\mathbf{c}}$/^{10}Be$_{\mathbf{c}}$ production ratio of 4.08 ± 0.37 (Balco and Shuster, 2009), yielding ^{21}Ne SLHL production rates of 18.4 ± 2.7 atoms g^{-1} yr^{-1} for high-energy neutrons, and 0.69 ± 0.19 atoms g^{-1} yr^{-1} for slow and fast muons respectively.

The results of the ^{10}Be$_{\mathbf{c}}$ analyses in the eight amalgamated sand samples are summarised in Fig. 1A and Table 1. Sample N1, collected from the trunk channel at the catchment outlet, yields a catchment-wide denudation rate of 9.6 ± 1.1 m Myr^{-1}. Tributary samples (N2A to N3C) yield catchment-wide denudation rates that range from 3.8 ± 0.4 to 16.9 ± 1.9 m Myr^{-1}. These rates are consistent with published data (Bierman and Caffee, 2001; Codilean et al., 2008) and confirm the strong relationship between denudation rate and mean catchment slope (Codilean et al., 2008) (Fig. 1B).

The results of the ^{10}Be$_{\mathbf{c}}$ and ^{26}Al$_{\mathbf{c}}$ analyses in the 15 pebbles are summarised in Table 2. The 15 pebbles were selected such that the whole range of ^{21}Ne concentrations obtained by Codilean et al. (2008) is covered (Fig. 1C). ^{10}Be$_{\mathbf{c}}$ and ^{26}Al$_{\mathbf{c}}$ concentrations span nearly two orders of magnitude: 0.22 ± 0.01 to 20.74 ± 0.52 × 10^{6} ^{10}Be atoms g^{-1} and 1.35 ± 0.09 to 72.76 ± 2.04 × 10^{6} ^{26}Al atoms g^{-1}. To allow for a first order comparison between the ^{10}Be$_{\mathbf{c}}$, ^{26}Al$_{\mathbf{c}}$, and ^{21}Ne$_{\mathbf{c}}$ data, without implying that such a procedure is appropriate with these data, we calculate catchment-wide denudation rates using the average of the nuclide concentrations in the pebbles, obtaining ~0.7, ~0.9, and ~0.8 m Myr^{-1} for ^{10}Be$_{\mathbf{c}}$, ^{26}Al$_{\mathbf{c}}$, and ^{21}Ne$_{\mathbf{c}}$, respectively. These values are virtually identical, and are one order of magnitude lower than that obtained from the amalgamated sand sample N1 from the catchment outlet, namely 9.6 ± 1.1 m Myr^{-1} (Fig. 1A).

Table 1
Summary of amalgamated sand ^{10}Be data. See text for details on denudation rate calculations.

ID	Longitude[b] (degrees)	Latitude (degrees)	Area (km^2)	Elevation (m)			Production scaling factors[c]			^{10}Be[d,e] 10^6 atoms g^{-1}	Denudation rate[e] m Myr^{-1}
				Min	Max	Mean	Spallation	Slow muons	Fast muons		
N1	16.090390	−23.480911	1264.53	940	2353	1573	2.15	2.07	1.09	0.767 ± 0.025	9.6 ± 1.1
N2A	16.089481	−23.478488	95.21	946	2351	1357	1.84	1.89	1.08	0.405 ± 0.014	16.6 ± 1.9
N2B	16.090390	−23.480911	81.28	940	1980	1335	1.82	1.87	1.08	0.393 ± 0.014	16.9 ± 1.9
N2C[a]	16.231486	−23.484712	45.77	1051	1938	1565	2.14	2.06	1.09	0.425 ± 0.016	18.0 ± 2.1
N2D	16.245457	−23.482986	19.68	1067	1938	1359	1.84	1.89	1.08	0.402 ± 0.022	16.7 ± 2.0
N2F	16.278043	−23.477074	73.80	1089	2187	1632	2.24	2.12	1.09	0.501 ± 0.016	15.8 ± 1.8
N2G[a]	16.313166	−23.469645	91.47	1119	2099	1619	2.19	2.10	1.09	0.493 ± 0.016	15.7 ± 1.7
N3A	16.459222	−23.365757	10.01	1728	1813	1764	2.42	2.24	1.10	1.916 ± 0.053	3.8 ± 0.4
N3B	16.434851	−23.387140	18.43	1674	1884	1751	2.40	2.22	1.10	1.286 ± 0.038	6.0 ± 0.7
N3C	16.433583	−23.357052	81.08	1717	1922	1817	2.51	2.29	1.11	1.243 ± 0.040	6.5 ± 0.7
N3E[a]	16.419892	−23.342974	48.44	1731	1916	1835	2.53	2.30	1.11	1.294 ± 0.042	6.3 ± 0.7
N3F[a]	16.344922	−23.325474	78.18	1770	2352	1867	2.60	2.33	1.11	0.904 ± 0.029	9.6 ± 1.1

[a] From Codilean et al. (2008).
[b] Longitude and latitude indicate the location of each catchment outlet on the 90 m SRTM DEM (http://srtm.csi.cgiar.org/); Values referenced to WGS84 datum.
[c] Combined altitude/latitude/topographic shielding scaling calculated following Dunai (2000) and Codilean (2006).
[d] Normalised to 2007 KNSTD standard (Nishiizumi et al., 2007), compatible with the updated ^{10}Be half-life of 1.387 ± 0.012 Myr (Chmeleff et al., 2010; Korschinek et al., 2010).
[e] Uncertainties at one-sigma level.

The plots in Fig. 3 indicate the presence of a relative excess of ^{21}Ne in six of the pebbles, namely, A1, A3, B6, C7, D0, and E1. These pebbles have $^{21}Ne_{\mathbf{c}}/^{10}Be_{\mathbf{c}}$ ratios that plot in the complex exposure/burial domain in Fig. 3B whereas with the exception of B6 and E1, the remaining pebbles have $^{26}Al_{\mathbf{c}}/^{10}Be_{\mathbf{c}}$ ratios that plot at one-sigma level within the erosion-island envelope in Fig. 3A. The latter indicates that the relatively high $^{21}Ne_{\mathbf{c}}/^{10}Be_{\mathbf{c}}$ ratios in the six pebbles are not the result of decay of $^{10}Be_{\mathbf{c}}$, but rather the result of the presence of a relative excess of non-cosmogenic ^{21}Ne. This excess of ^{21}Ne however, is of minor importance for explaining the grain size bias observed in the Gaub River catchment given the first order agreement between the average abundances of the three nuclides. In this study we focus on the $^{10}Be_{\mathbf{c}}$ and $^{26}Al_{\mathbf{c}}$ results only, and will later discuss the geochemical subtleties of the ^{21}Ne in the Gaub pebbles elsewhere.

4. Discussion and concluding remarks

Neither the presence of substantial unaccounted-for non-cosmogenic ^{21}Ne in the pebbles nor radioactive decay of $^{10}Be_{\mathbf{c}}$ during long-term sediment storage is the likely cause of the grain-size effect observed in the Gaub. The first order agreement between the three nuclides in the pebbles and the order-of-magnitude difference in $^{10}Be_{\mathbf{c}}$ between the pebbles and the amalgamated sand, indicate that the pebbles cannot contain the substantial amounts of non-cosmogenic ^{21}Ne necessary to explain the difference between the nuclide inventories of the two size fractions. Moreover, burial during long-term sediment storage would result in decay of $^{10}Be_{\mathbf{c}}$ and $^{26}Al_{\mathbf{c}}$ in both size fractions. The $^{26}Al_{\mathbf{c}}/^{10}Be_{\mathbf{c}}$ ratios in the pebbles do not indicate obvious complex exposure histories, with all but three of the samples either intersecting at one-sigma or falling completely within the erosion-island envelope in Fig. 3A. Thus, burial and storage at depth of the pebbles have very likely not been substantial.

Two remaining mechanisms could explain the covariance between grain size and the cosmogenic nuclide concentrations observed in the Gaub. The first involves substantially longer sediment transport times for the pebbles than for the sand-sized grains. Longer transport times would mean longer exposure to cosmic radiation and thus higher nuclide concentrations in the pebbles. This mechanism is problematic for the Gaub, however. Firstly, the relatively high nuclide concentrations measured in the pebbles can be reproduced by measured bedrock erosion rates alone, and they do not require cosmogenic nuclide acquisition during transport through the drainage system (Codilean et al., 2008). Secondly, a simple calculation suggests that a difference in transport times on the order of 10^5 years is necessary to produce the order-of-magnitude difference in nuclide concentrations between the two size fractions (see also Codilean et al., 2010). Given the small catchment size and lack of both accommodation space and sediment in storage, such long sediment residence times are unlikely for arid catchments such as the Gaub.

A second mechanism for explaining the apparent inconsistency between the $^{10}Be_{\mathbf{c}}$ and $^{26}Al_{\mathbf{c}}$ in the pebbles and the $^{10}Be_{\mathbf{c}}$ in the amalgamated sand is that of differential sediment sourcing. The average of the denudation rates obtained for the 11 Gaub tributary sand samples (Fig. 1A) is 12.0 ± 1.7 m Myr^{-1}, overlapping at one sigma with that obtained from sample N1, collected at the catchment outlet (9.6 ± 1.1 m Myr^{-1}). This equivalence demonstrates that the sediment leaving the study catchment is well mixed and all areas of the catchment contribute to the total mix at the outlet. Thus, the amalgamated sands leaving the catchment are an aggregate of grains originating from quartz-bearing rocks in all

Table 2
Summary of individual pebble ^{10}Be and ^{26}Al data.

ID[a]	Nuclide concentration (10^6 atoms g^{-1})	
	^{10}Be[b,c]	^{26}Al[c]
A0	10.545 ± 0.264	53.760 ± 1.510
A1	0.960 ± 0.030	6.308 ± 0.246
A3	1.376 ± 0.034	8.401 ± 0.295
A6	8.034 ± 0.201	42.080 ± 1.173
B2	6.615 ± 0.193	35.290 ± 0.990
B6	1.083 ± 0.036	6.123 ± 0.220
C4	20.743 ± 0.518	72.760 ± 2.035
C7	0.689 ± 0.022	4.562 ± 0.191
D0	0.216 ± 0.013	1.348 ± 0.093
D1	4.035 ± 0.113	24.650 ± 0.845
D8	1.850 ± 0.049	12.130 ± 0.444
E1	0.325 ± 0.014	1.712 ± 0.084
E3	11.650 ± 0.291	53.340 ± 1.494
E8	11.248 ± 0.281	36.950 ± 1.069
F7	11.778 ± 0.295	49.510 ± 1.392

[a] Location information same as for sample N1.
[b] Normalised to 2007 KNSTD standard (Nishiizumi et al., 2007), compatible with the updated ^{10}Be half-life of 1.387 ± 0.012 Myr (Chmeleff et al., 2010; Korschinek et al., 2010).
[c] Uncertainties at one-sigma level.

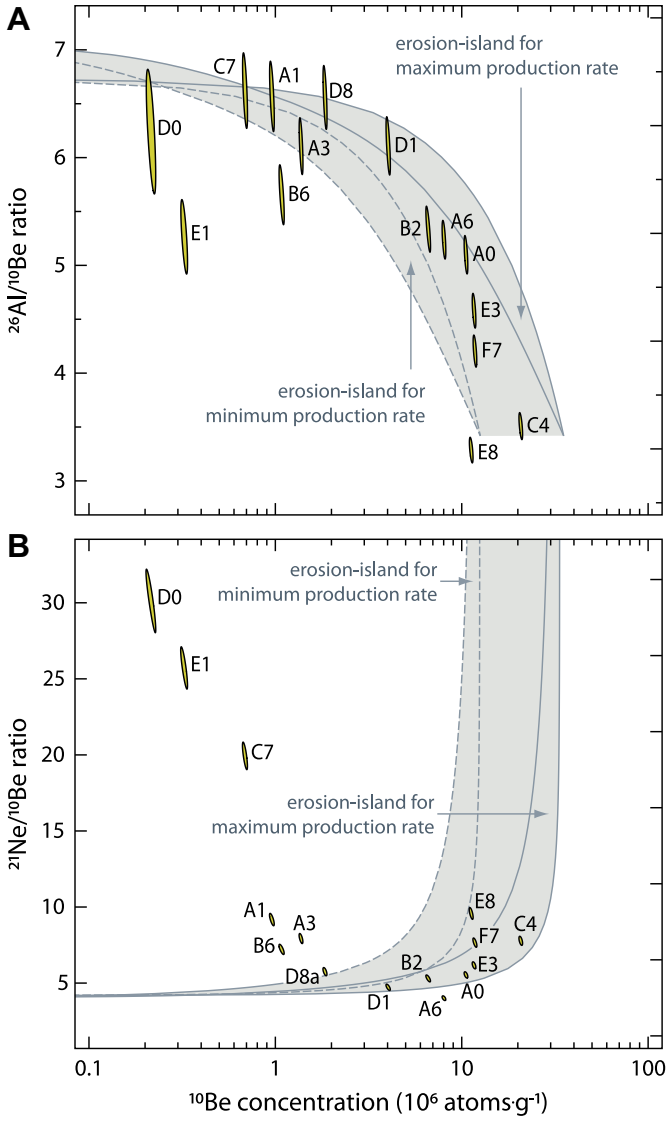

Fig. 3. Plots showing the $^{26}Al_c/^{10}Be_c$ and $^{21}Ne_c/^{10}Be_c$ ratios ($\pm 1\sigma$) vs. $^{10}Be_c$ concentration in the 15 pebbles. Pebbles that have been exposed continuously to cosmic radiation (i.e., no burial) should plot within the erosion-island envelope defined as the grey area between the erosion-island plots for the minimum and maximum cosmogenic nuclide production rates in the study catchment. Points plotting below or above the erosion-island envelope indicate either a complex exposure history (i.e., at least one episode of burial) or measurement error, respectively, for that sample.

parts of the catchment, and the cosmogenic nuclide inventories of these sands record the overall average lowering rate of the landscape.

Unlike the surrounding bedrock that disintegrates into sand-sized grains, quartz-vein outcrops tend to break up episodically into larger clasts (Fig. 2) (cf. Small et al., 1997; Muzikar, 2008, 2009). We infer that the pebbles originate from the quartz-vein outcrops throughout the catchment, and the episodic erosion of the latter means that the pebbles have higher nuclide inventories than the surrounding bedrock and soil, and therefore also higher than the amalgamated sand grains (Figs. 4 and 5). These quartz-vein outcrops, although ubiquitous, constitute only a minute percentage of the overall land surface in the study catchment, and so, despite higher nuclide concentrations, the cosmogenic 'signal' from quartz vein-sourced sand grains (derived presumably by break-down of larger clasts such as the pebbles we sampled) is diluted as they contribute only a small fraction of total cosmogenic nuclide concentration in the exported sediment. This second mechanism is supported by published data (Bierman and Caffee, 2001; Bierman et al., 2007; Cockburn et al., 2000; Codilean et al., 2008; van der Wateren and Dunai, 2001). Fig. 6, a summary of all cosmogenic nuclide data from bedrock and amalgamated sand samples collected in central-western Namibia, indicates that amalgamated sand samples record higher erosion rates than their bedrock counterparts, and that quartz-vein outcrops account for the majority of the lowest measured bedrock erosion rates for this area.

It is unlikely, however, that the second mechanism described above can alone explain the order-of-magnitude difference between the cosmogenic nuclide inventories of the amalgamated sands and individual pebbles, as this would require long time intervals between successive quartz-vein outcrop spalling events, and thus unrealistically tall outcrops. The latter is not observed in the field. It is more likely that the order-of-magnitude grain size bias observed in the Gaub is a result of the combined effects of both mechanisms described here (Fig. 5). Pebbles accumulate more cosmogenic nuclides than finer grains because of the episodic nature of the erosion of their source quartz-vein outcrops, and because they also spend relatively longer amounts of time in transport on the hillslopes than do sand grains, simply because the hydrological events that mobilise larger clasts occur more rarely than those that mobilise sand.

Independent of the cause, however, the order-of-magnitude grain size bias observed in the Gaub has important implications

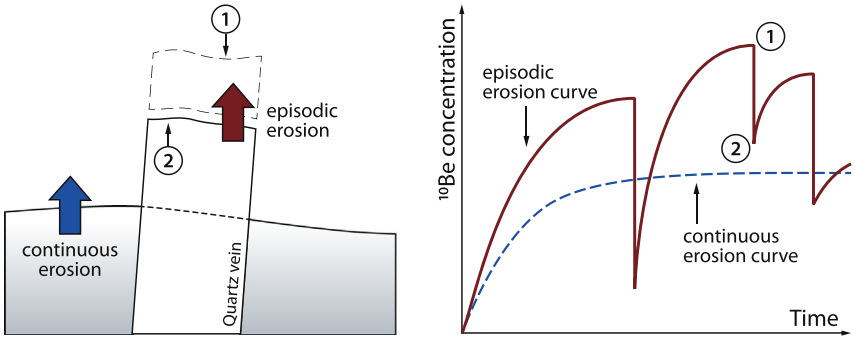

Fig. 4. Accumulation of $^{10}Be_c$ in an eroding surface under continuous erosion (blue) and episodic erosion (red). Under continuous steady erosion the surface $^{10}Be_c$ concentration reaches a constant value (dashed blue curve), and the amount of $^{10}Be_c$ produced by cosmic rays equals the amount removed by erosion and radioactive decay. Episodic erosion processes, on the other hand, result in the removal of discrete blocks of rock. The truncation of the exponentially decreasing $^{10}Be_c$ depth-profile means that a constant surface $^{10}Be_c$ concentration is never reached; instead the surface concentration fluctuates with time (red curve) as the amount of $^{10}Be_c$ produced never equals the amount removed by erosion. Under these conditions, the material removed by spalling of blocks from an outcropping quartz vein has a higher $^{10}Be_c$ concentration (1) than the quartz-vein surface that becomes exposed (2). In addition to eroding episodically, a quartz vein outcrop is also exposed to cosmic radiation from all directions and so, material removed (e.g., quartz pebbles) will likely have a higher $^{10}Be_c$ concentration than the surrounding landscape that is both eroding continuously (dashed blue curve) and is only exposed to cosmic radiation from above. Based on Small et al. (1997) and Muzikar (2008, 2009). (For interpretation of the references to colour in this figure legend, the reader is referred to the web version of this article.)

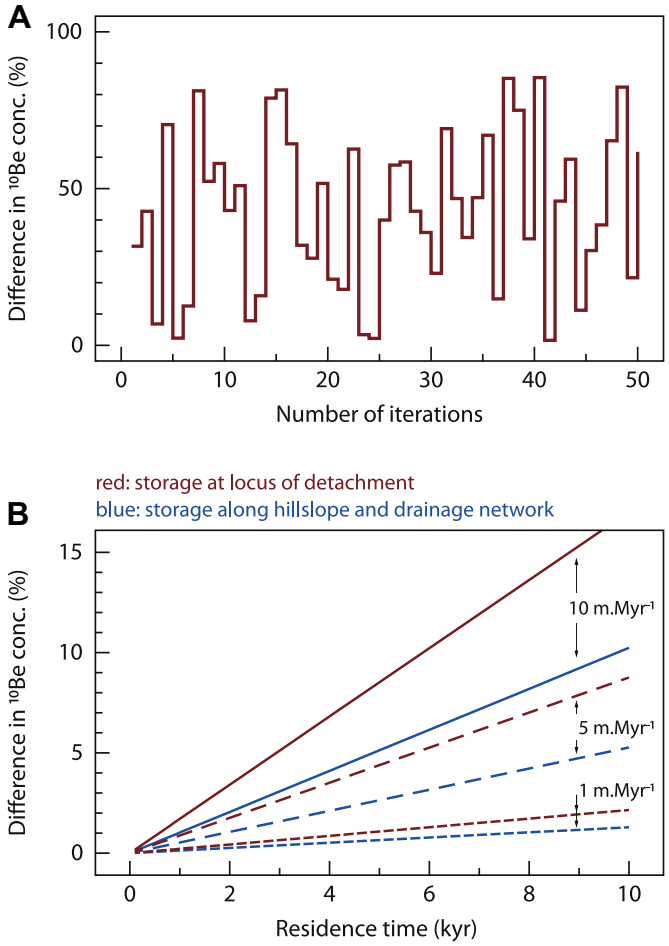

Fig. 5. (A) Numerical simulation showing the temporal evolution of the $^{10}Be_c$ concentration at the top of a quartz-vein outcrop (labelled (1) in Fig. 4) that is eroded by the episodic spalling of blocks, as compared to the $^{10}Be_c$ concentration of the surrounding bedrock/soil that is subject to continuous erosion. In the simulation, the quartz-vein outcrop's maximum permissible height is 50 cm. At each iteration the outcrop is truncated by removing a block of random thickness between 0 and 50 cm. (B) Plot showing the % increase in the $^{10}Be_c$ concentration of pebbles as a result of longer sediment transport times, as compared to the $^{10}Be_c$ concentration of their source. The relative increase in the $^{10}Be_c$ concentration of pebbles depends on (1) their $^{10}Be_c$ at detachment, and therefore the erosion rate of their source, and (2) the elevations at which the pebbles are exposed to cosmic radiation during their transport through the catchment.

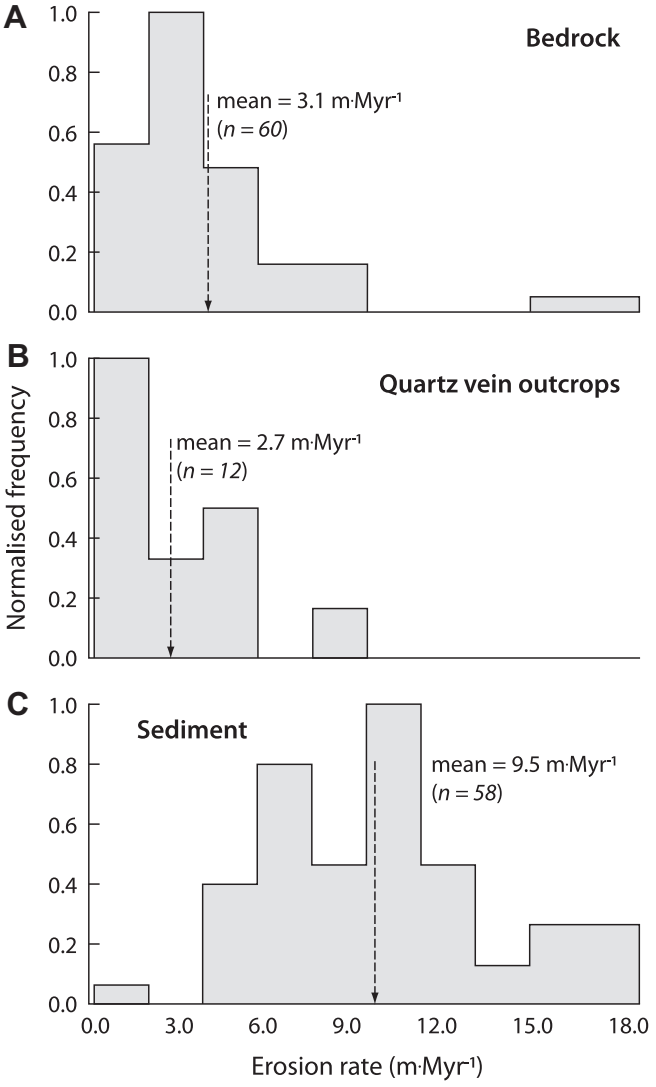

Fig. 6. Frequency distribution plots summarising $^{10}Be_c$-based erosion rates obtained for central-western Namibia from bedrock and amalgamated sand samples by Cockburn et al. (2000), Bierman and Caffee (2001), van der Wateren and Dunai (2001), Bierman et al. (2007), Codilean et al. (2008), and this study. Frequency distribution plots show rates inferred from: (A) exposed bedrock excluding those samples where quartz-vein outcrops were sampled. Note that the large frequency in the first bin is partly the result of including Cockburn et al.'s (2000) samples collected from the summit of the Gamsberg, a flat-topped granite residual capped by a ~25 m thick quartzite unit that yielded erosion rates ~0.6 m Myr^{-1}; (B) Quartz-vein outcrops. Note the high skew towards low values suggesting that quartz-vein outcrops account for the majority of the lowest recorded rates in central-western Namibia; (C) Amalgamated sand.

for using cosmogenic nuclide abundances in depositional surfaces to quantify palaeo-denudation rates in arid environments akin to our study catchment in Namibia. Analyses of the distribution of cosmogenic nuclide concentrations in depth profiles on depositional surfaces such as fluvial terraces are useful for simultaneously determining both the depositional age of the surface and the palaeo-denudation rate that characterised the landscape prior to the deposition of the dated sediment (Anderson et al., 1996; Braucher et al., 2009; Hidy et al., 2010). Amalgamated clasts are often preferred to sand-sized material for these studies mainly because they are less likely to be re-mobilised after deposition (Repka et al., 1997). The principle behind the method is that the cosmogenic nuclide concentration of each amalgamated clast sample in the depth profile is the sum of two components: (1) a post-depositional component reflecting the depositional age and the rate of erosion of the depositional surface, and (2) an inherited component reflecting the denudation rate prior to the deposition of the samples. The first component is acquired exclusively after deposition and so the age and erosion rate of the depositional surface are not affected by a covariance between cosmogenic nuclide activity and grain size. Determination of the palaeo-denudation rate, on the other hand, depends on the absolute cosmogenic nuclide concentrations in the depth profile samples, and so it will be affected by a grain size bias. In environments akin to our study catchment, pebble-sized clasts will yield substantially underestimated palaeo-denudation rates.

Acknowledgements

The ^{10}Be and ^{26}Al measurements were funded by the UK Natural Environment Research Council Cosmogenic Isotope Analysis Facility Allocation No. 9054.0408. This study was prompted by

discussions with Paul Bierman and Roderick Brown. Constructive comments on a previous version of this manuscript by Darryl Granger and Pieter Vermeesch are acknowledged. Constructive reviews by Kevin Norton, Ari Matmon, and an anonymous reviewer are also acknowledged.

Editorial handling by: N. Akçar

Appendix A. Supplementary material

Supplementary data associated with this article can be found, in the online version, at doi:10.1016/j.quageo.2012.04.007.

References

Anderson, R.S., Repka, J.L., Dick, G.S., 1996. Explicit treatment of inheritance in dating depositional surfaces using in situ ^{10}Be and ^{26}Al. Geology 24, 47–51. doi:10.1130/0091-7613(1996)024<0047:ETOIID>2.3.CO;2.

Balco, G., Shuster, D.L., 2009. Production rate of cosmogenic ^{21}Ne in quartz estimated from ^{10}Be, ^{26}Al, and ^{21}Ne concentrations in slowly eroding Antarctic bedrock surfaces. Earth and Planetary Science Letters 281, 48–58. doi:10.1016/j.epsl.2009.02.006.

Balco, G., Stone, J.O., Lifton, N.A., Dunai, T.J., 2008. A complete and easily accessible means of calculating surface exposure ages or erosion rates from ^{10}Be and ^{26}Al measurements. Quaternary Geochronology 3, 174–195. doi:10.1016/j.quageo.2007.12.001.

Belmont, P., Pazzaglia, F.J., Gosse, J.C., 2007. Cosmogenic ^{10}Be as a tracer for hillslope and channel sediment dynamics in the Clearwater River, western Washington State. Earth and Planetary Science Letters 264, 123–135. doi:10.1016/j.epsl.2007.09.013.

Bierman, P.R., Caffee, M., 2001. Slow rates of rock surface erosion and sediment production across the Namib Desert and Escarpment, Southern Africa. American Journal of Science 301, 326–358. doi:10.2475/ajs.301.4-5.326.

Bierman, P.R., Steig, E.J., 1996. Estimating rates of denudation using cosmogenic isotope abundances in sediment. Earth Surface Processes and Landforms 21, 125–139. doi:10.1002/(sici)1096-9837(199602)21:2<125::aid-esp511>3.0.co;2-8.

Bierman, P.R., Nichols, K.K., Matmon, A., Enzel, Y., Larsen, J., Finkel, R., 2007. ^{10}Be shows that Namibian drainage basins are slowly, steadily and uniformly eroding. Quaternary International 167–168, 33.

Braucher, R., del Castillo, P., Siame, L.L., Hidy, A.J., Bourles, D.L., 2009. Determination of both exposure time and denudation rate from an in situ-produced ^{10}Be depth profile: a mathematical proof of uniqueness. Model sensitivity and applications to natural cases. Quaternary Geochronology 4, 56–67. doi:10.1016/j.quageo.2008.06.001.

Brown, E.T., Stallard, R.F., Larsen, M.C., Bourles, D.L., Raisbeck, G.M., Yiou, F., 1998. Determination of predevelopment denudation rates of an agricultural watershed (Cayaguas River, Puerto Rico) using in-situ-produced ^{10}Be in river-borne quartz. Earth and Planetary Science Letters 160, 723–728. doi:10.1016/s0012-821x(98)00123-x.

Brown, E.T., Stallard, R.F., Larsen, M.C., Raisbeck, G.M., Yiou, F., 1995. Denudation rates determined from the accumulation of in situ-produced ^{10}Be in the Luquillo Experimental Forest, Puerto Rico. Earth and Planetary Science Letters 129, 193–202. doi:10.1016/0012-821x(94)00249-x.

Chmeleff, J., von Blanckenburg, F., Kossert, K., Jakob, D., 2010. Determination of the ^{10}Be half-life by multicollector ICP-MS and liquid scintillation counting. Nuclear Instruments and Methods in Physics Research Section B 268, 192–199. doi:10.1016/j.nimb.2009.09.012.

Clapp, E.M., Bierman, P.R., Caffee, M.W., 2002. Using ^{10}Be and ^{26}Al to determine sediment generation rates and identify sediment source areas in an arid region drainage basin. Geomorphology 45, 89–104. doi:10.1016/S0169-555X(01)00191-X.

Clapp, E.M., Bierman, P.R., Schick, A.P., Lekach, J., Enzel, Y., Caffee, M.W., 2000. Sediment yield exceeds sediment production in arid region drainage basins. Geology 28, 995–998. doi:10.1130/0091-7613(2000)28<995:syespi>2.0.co;2.

Cockburn, H.A.P., Brown, R.W., Summerfield, M.A., Seidl, M.A., 2000. Quantifying passive margin denudation and landscape development using a combined fission-track thermochronology and cosmogenic isotope analysis approach. Earth and Planetary Science Letters 179, 429–435. doi:10.1016/s0012-821x(00)00144-8.

Codilean, A.T., 2006. Calculation of the cosmogenic isotope production topographic shielding scaling factor for large areas using DEMs. Earth Surface Processes and Landforms 31, 785–794. doi:10.1002/esp.1336.

Codilean, A.T., Bishop, P., Hoey, T.B., Stuart, F.M., Fabel, D., 2010. Cosmogenic ^{21}Ne analysis of individual detrital grains: opportunities and limitations. Earth Surface Processes and Landforms 35, 16–27. doi:10.1002/esp.1815.

Codilean, A.T., Bishop, P., Stuart, F.M., Hoey, T.B., Fabel, D., Freeman, S.P.H.T., 2008. Single-grain cosmogenic ^{21}Ne concentrations in fluvial sediments reveal spatially variable erosion rates. Geology 36, 159–162. doi:10.1130/g24360a.1.

Dunai, T.J., 2000. Scaling factors for production rates of in situ produced cosmogenic nuclides: a critical reevaluation. Earth and Planetary Science Letters 176, 157–169. doi:10.1016/S0012-821X(99)00310-6.

Dunai, T.J., 2010. Cosmogenic Nuclides: Principles, Concepts and Applications in the Earth Surface Sciences. Cambridge University Press. doi:10.1017/CBO9780511804519, p. 198.

Freeman, S.P.H.T., Bishop, P., Bryant, C., Cook, G., Dougans, D., Ertunc, T., Fallick, A., Ganeshram, R., Maden, C., Naysmith, P., Schnabel, C., Scott, M., Summerfield, M., Xu, S., 2007. The SUERC AMS laboratory after 3 years. Nuclear Instruments and Methods in Physics Research B 259, 66–70. doi:10.1016/j.nimb.2007.01.312.

Freeman, S.P.H.T., Bishop, P., Bryant, C., Cook, G., Fallick, A., Harkness, D., Metcalfe, S., Scott, M., Scott, R., Summerfield, M., 2004. A new environmental sciences AMS laboratory in Scotland. Nuclear Instruments and Methods in Physics Research B 31, 223–224. doi:10.1016/j.nimb.2004.04.010.

Granger, D.E., Kirchner, J.W., Finkel, R., 1996. Spatially averaged long-term erosion rates measured from in situ − produced cosmogenic nuclides in alluvial sediment. The Journal of Geology 104, 249–257.

Heisinger, B., Lal, D., Jull, T.A.J., Kubik, P.W., Ivy-Ochs, S., Neumaier, S., Knie, K., Lazarev, V., Nolte, E., 2002a. Production of selected cosmogenic radionuclides by muons 1. Fast Muons: Earth and Planetary Science Letters 200, 345–355. doi:10.1016/S0012-821X(02)00640-4.

Heisinger, B., Lal, D., Jull, T.A.J., Kubik, P.W., Ivy-Ochs, S., Knie, K., Nolte, E., 2002b. Production of selected cosmogenic radionuclides by muons: 2. Capture of Negative Muons: Earth and Planetary Science Letters 200, 357–369. doi:10.1016/S0012-821X(02)00641-6.

Hidy, A.J., Gosse, J.C., Pederson, J.L., Mattern, J.P., Finkel, R.C., 2010. A geologically constrained Monte Carlo approach to modeling exposure ages from profiles of cosmogenic nuclides: an example from Lees Ferry, Arizona. Geochemistry Geophysics Geosystems 11, Q0AA10. doi:10.1029/2010GC003084.

Korschinek, G., Bergmaierb, A., Faestermanna, T., Gerstmannc, U.C., Kniea, K., Rugela, G., Wallnerd, A., Dillmanna, I., Dollingerb, G., Lierse von Gostomskie, Ch., Kossertf, K., Maitia, M., Poutivtseva, M., Remmer, A., 2010. A new value for the half-life of ^{10}Be by heavy ion elastic recoil detection and liquid scintillation counting. Nuclear Instruments and Methods in Physics Research Section B 268, 187–191. doi:10.1016/j.nimb.2009.09.020.

Kubik, P.W., Christl, M., Alfimov, V., 2009. New Primary ^{10}Be Standard and T1/2 for AMS at ETH: Ion Beam Physics, ETH Zurich Annual Report, p. 12.

Maden, C., Anastasi, P.A.F., Dougans, A., Freeman, S.P.H.T., Kitchen, R., Klody, G., Schnabel, C., Sundquist, M., Vanner, K., Xu, S., 2007. SUERC AMS ion detection. Nuclear Instruments and Methods in Physics Research B 259, 131–139. doi:10.1016/j.nimb.2007.01.151.

Matmon, A., Bierman, P.R., Larsen, J., Southworth, S., Pavich, M., Finkel, R., Caffee, M., 2003. Erosion of an ancient mountain range, the Great Smoky Mountains, North Carolina and Tennessee. American Journal of Science 303, 817–855,. doi:10.2475/ajs.303.9.817.

Middleton, R., Brown, L., Dezfouly-Arjomandy, B., Klein, J., 1993. On ^{10}Be standards and the half-life of ^{10}Be. Nuclear Instruments and Methods in Physics Research B 82, 399–403. doi:10.1016/0168-583X(93)95987-G.

Muzikar, P., 2008. Cosmogenic nuclide concentrations in episodically eroding surfaces: Theoretical results. Geomorphology 97, 407–413. doi:10.1016/j.geomorph.2007.08.020.

Muzikar, P., 2009. General models for episodic surface denudation and its measurement by cosmogenic nuclides. Quaternary Geochronology 4, 50–55. doi:10.1016/j.quageo.2008.06.004.

Niedermann, S., 2002. Cosmic-ray-produced noble gases in terrestrial rocks: dating tools for surface processes. In: Porcelli, D.P., Ballentine, C.J., Wieler, R. (Eds.), 2002. Noble Gases: Reviews in Mineralogy and Geochemistry, vol. 47, pp. 731–784. doi:10.2138/rmg.2002.47.16.

Nishiizumi, K., 2002, ^{10}Be, ^{26}Al, ^{36}Cl and ^{41}Ca standards: Ninth International Conference on Accelerator Mass Spectrometry (AMS-9), Nagoya, Japan, Abstracts.

Nishiizumi, K., 2004. Preparation of ^{26}Al AMS standards. Nuclear Instruments and Methods in Physics Research B 223–224, 388–392. doi:10.1016/j.nimb.2004.04.075.

Nishiizumi, K., Imamura, M., Caffee, M.W., Southon, J.R., Finkel, R.C., McAninch, J., 2007. Absolute calibration of ^{10}Be AMS standards. Nuclear Instruments and Methods in Physics Research B 259, 403–413. doi:10.1016/j.nimb.2007.01.297.

Ouimet, W.B., Whipple, K.X., Granger, D.E., 2009. Beyond threshold hillslopes: channel adjustment to base-level fall in tectonically active mountain ranges. Geology 37, 579–582. doi:10.1130/G30013A.1.

Palumbo, L., Hetzel, R., Tao, M., Li, X., 2010. Topographic and lithologic control on catchment-wide denudation rates derived from cosmogenic ^{10}Be in two mountain ranges at the margin of NE Tibet. Geomorphology 117, 130–142. doi:10.1016/j.geomorph.2009.11.019.

Portenga, E.W., Bierman, P.R., 2011. Understanding Earth's eroding surface with ^{10}Be. GSA Today 21, 4–10. doi:10.1130/G111A.1.

Repka, J., Anderson, R.S., Finkel, R.C., 1997. Cosmogenic dating of fluvial terraces, Fremont River, Utah. Earth and Planetary Science Letters 152, 59–73. doi:10.1016/S0012-821X(97)00149-0.

Roberts, D.H., Long, A.J., Schnabel, C., Freeman, S.P.H.T., Simpson, M.J.R., 2008. The deglacial history of the southeast sector of the Greenland Ice Sheet during the Last Glacial maximum. Quaternary Science Reviews 27, 1505–1516. doi:10.1016/j.quascirev.2008.04.008.

Schaller, M., von Blanckenburg, F., Hovius, N., Kubik, P.W., 2001. Large-scale erosion rates from in situ-produced cosmogenic nuclides in European river sediments.

Earth and Planetary Science Letters 188, 441–458. doi:10.1016/s0012-821x(01)00320-x.

Schnabel, C., Reinhardt, L., Barrows, T.T., Bishop, P., Davidson, A., Fifield, L.K., Freeman, S., Kim, J.Y., Maden, C., Xu, S., 2007. Inter-comparison in ^{10}Be analysis starting from pre-purified quartz. Nuclear Instruments and Methods in Physics Research B 259, 571–575. doi:10.1016/j.nimb.2007.01.298.

Small, E., Anderson, R.S., Repka, J.L., Finkel, R.C., 1997. Erosion rates of alpine bedrock summit surfaces deduced from in situ ^{10}Be and ^{26}Al. Earth and Planetary Science Letters 150, 413–425. doi:10.1016/S0012-821X(97)00092-7.

van der Wateren, F.M., Dunai, T.J., 2001. Late Neogene passive margin denudation history-cosmogenic isotope measurements from the central Namib desert. Global and Planetary Change 30, 271–307. doi:10.1016/s0921-8181(01)00104-7.

von Blanckenburg, F., 2005. The control mechanisms of erosion and weathering at basin scale from cosmogenic nuclides in river sediment. Earth and Planetary Science Letters 237, 462–479. doi:10.1016/j.epsl.2005.06.030.

Wilson, P., Bentley, M., Schnabel, C., Clark, R., Xu, S., 2008. Stone run (block stream) formation in the Falkland Islands over several cold stages, deduced from cosmogenic isotope (^{10}Be and ^{26}Al) surface exposure dating. Journal of Quaternary Science 23, 461–473. doi:10.1002/jqs.1156.

Wittmann, H., von Blanckenburg, F., Maurice, L., Guyot, J.L., Filizola, N., Kubik, P.W., 2011. Sediment production and delivery in the Amazon River basin quantified by in situ-produced cosmogenic nuclides and recent river loads. Geological Society of America Bulletin 123, 934–950. doi:10.1130/B30317.1.

Xu, S., Dougans, A.B., Freeman, S.P.H.T., Schnabel, C., Wilcken, K.M., 2010. Improved ^{10}Be and ^{26}Al AMS with a 5 MV spectrometer. Nuclear Instruments and Methods in Physics Research B 268, 736–738. doi:10.1016/j.nimb.2009.10.018.

Ziegler, U.R.F., Stoessel, G.F.U., 1993. Age determinations in the Rehoboth Basement Inlier, Namibia. Geological Survey of Namibia Memoir 14, 106.